Heliyon 7 (2021) e06569

Contents lists available at ScienceDirect

Heliyon

journal homepage: www.cell.com/heliyon

Research article

Effect of supercapacitors on the operation of an air-cooled hydrogen fuel cell

Ashleigh Townsend [a,*], Christiaan Martinson [b], Rupert Gouws [a], Dmitri Bessarabov [b]

[a] School of Electrical, Electronic and Computer Engineering, North West University, Potchefstroom 2520, South Africa
[b] DST HySA Infrastructure Center of Competence, Faculty of Engineering, North West University, Potchefstroom 2520, South Africa

ARTICLE INFO

Keywords:
Fuel cell
Supercapacitor
Unmanned aerial vehicle
Fuel cell hybrid
Supercapacitor hybrid

ABSTRACT

One of the greatest challenges associated with efficient energy use in unmanned aerial vehicles (drones) is that of the energy storage systems – more specifically it's weight and capacity. Current hydrogen fuel cell drones have very promising flight durations, but have a low power density thus performing poorly at peak power demands. Supercapacitors are known to have high power densities and respond significantly well to peak power demands. For this research it is desired to evaluate how supercapacitors can affect the operation of an existing hydrogen fuel cell system, when combined. This study will include the evaluation of the viability of a DC-DC converter used to reduce the size (and subsequently, weight) of a supercapacitor bank. It also evaluates whether specified switching of the sources has an effect. Using data generated from the experiment it was determined that the DC-DC converter (with efficiency >94%) reduced the efficiency (by 0.5%) and duration (by 3.8%) of the supercapacitor bank whilst increasing the weight (by 16.7%). It was also seen that the method of selective switching offered no benefit over that of a self-selecting system, where the former obtained 223 s of usability and the latter 365 s. However, comparing all the results it was observed that the addition of a supercapacitor bank allowed for an improvement in energy- and power density, of the hydrogen fuel cell system, from 0.65 Wh/kg to 1.19 Wh/kg and from 69.7 W/kg to 125.7 W/kg, respectively.

1. Introduction

Since drones have become more prevalent, many researchers have been evaluating the efficiency of drones and methods to increase the flight times thereof [1, 2]. There are mainly two options in achieving this goal: replace the power source with one of a greater capacity, or refuel the power source sporadically [3, 4]. The latter requires the use of refueling stations, which, in itself, presents more problems—the unmanned aerial vehicle (UAV) will be required to land periodically and refuel throughout its flight, decreasing the actual usable flight time [5]; stations will be required along the flight path, limiting the range and path, subsequently decreasing the mobility and increasing complexity [6]. These aspects all contribute to increasing the overall costs, unnecessarily. The former option in increasing the flight time offers more possibilities that could be simpler to implement and ultimately more cost effective. Some such possibilities include the following: increasing the capacity by replacing the original power source with one of a greater capacity or combining the existing power source with another to exploit the benefits of both (i.e., hybridization). However, all these options do have their respective advantages and disadvantages [7].

The Ragone plot reported by Aravindan et al. [8] depicts the energy and power densities of selected energy sources. This Ragone plot assists in providing a better understanding of why some sources are preferred over others. The power density refers to the amount of power contained within the volume capacity of a source that it can provide at a specific instance, whereas the energy density refers to the energy (Wh) contained within the volume capacity of a source, therefore, how long it can provide a specific amount of power. From this figure [8], the following are evident: supercapacitors (SCs) can provide a large amount of power (80–75 000 W/kg) but for a short period of time (energy density 0.9–0.1 Wh/kg), while hydrogen fuel cells (HFCs) can provide a small amount of power (1.5–20 W/kg) for a longer period of time (energy density 200–3000 Wh/kg). Furthermore, lithium ion (Li-ion) batteries are similar to HFCs as they too can provide a small amount of power (15–400 W/kg) for relatively long periods of time (energy density 20–150 Wh/kg) [8].

Currently, the demand for UAVs is mainly consumed by military applications, however, in recent years the demand in commercial, recreational and public applications has increased tenfold, and it is expected to exponentially shift further in this direction [9, 10]. The

* Corresponding author.
E-mail address: ashleighktownsend2@gmail.com (A. Townsend).

https://doi.org/10.1016/j.heliyon.2021.e06569
Received 5 January 2021; Received in revised form 25 February 2021; Accepted 17 March 2021

use of UAVs in criminal, theft and poaching surveillance is one of the major applications [11], with other applications including scientific monitoring (water sampling, landslides, volcanic activity) and transmission line surveillance [12, 13, 14, 15]. At present, combustion engines remain the most popular power supply for UAVs. Yet electrical systems offer a higher efficiency, can be more reliable, they have low to no greenhouse gas emissions and minimal noise [16]—clearly indicating why these systems are becoming more prevalent.

There are many different power sources available on the market such as, batteries, solar power, HFCs, combustion engines, amongst others [17], most of which can be applied to UAVs. Over the years, some of these power sources have been disregarded because, regarding this specific application, they have more disadvantages than advantages, for example, having a weight/size that is too large, being restricted to specific movements, or simply not having sufficient energy density.

Fuel cells offer several advantages, including the following: no direct pollution and no sound, with the refuel/recharge time of a HFC only limited to the availability of hydrogen in the environment and the speed of the acquisition of the hydrogen [18]. According to Schroth et al. [19], a HFC, compared to an equivalent lithium polymer (LiPo) battery, can have an energy density increase by a factor of 150 which is also superior to a gasoline-powered UAV. However, a HFC has the disadvantage of a lower power density in comparison to a gasoline-powered UAV, meaning that peak power requirements drain the HFC significantly, hence limiting applications and flight times [18, 20].

HFCs are often combined with LiPo batteries to improve the power density; however, batteries can have a similarly low power density [19]. Thus, although the addition of a battery can increase the endurance of the system and improve peak power performance, the increase is not to the desired point. Furthermore, both power supplies are still significantly drained during these peak power instances—thus still limiting the flight time of the system.

SCs have a very large energy capability, with a fast release aspect. This means that they can provide very large amounts of current over very short periods of time. However, SCs are very large in size (and weight) when compared to LiPo batteries of equivalent capabilities, thus making drones quite large in size. Although SCs have low energy densities, in comparison to batteries, they offer quick bursts of energy during peak power demands and can store energy quickly that would otherwise be lost [20]. Thus, the addition of SCs to any of the energy sources mentioned should lead to much better efficiencies of UAVs, especially during peak power requirements. SCs are relatively new, therefore they are still quite expensive and little research has been carried out into their application in combination with HFCs.

The HFC available to this project is currently being used in combination with a LiPo battery of similar power- and energy density. It was thus seen as beneficial to examine how the use of SCs can affect the functionality of this HFC system. The aim was to investigate this hybrid combination, with the future desire to replace the power source of a HFC UAV. Specific aspects focused on: determining the effect of the use of a DC-DC converter in conjunction with the SC bank, determining the effect of SCs on the operation of a HFC and determining the effect of selective switching and power source connection order on the operation of the hybrid combination.

2. Materials, methods and calculations

This project entails the design and build of an experimental setup to be used to test a proposed solution to a highlighted problem – combining multiple sources with various energy- and power densities to improve the characteristics of the energy source for eventual use in and improvement of a drone flight. For this it is necessary to discuss the setup of the experiment, the power sources to be used and the configuration of their use. These will be discussed below.

2.1. Hydrogen fuel cell hybridization case studies

To combine the power sources it is necessary to first determine how previous combinations were made and what the results and recommendations from those previous experiments were. This is done using case studies discussed below.

2.1.1. Hydrogen fuel cell and battery combination

Many studies have been done using this particular type of combination, these case studies will be used to assess the specific energy management of each as well as the outcomes and suggested improvements. Bauman et al. [21] utilizes a 35 kW HFC is combined with a Li-ion battery of 346.5 V, where the HFC utilizes a DC-DC converter in order to boost the voltage to (250–400 V) in order to use a smaller HFC to reduce costs and vehicle mass; the battery, however, does not use a converter as it delivers the required voltage. In this study the battery stores regenerative braking energy (when battery is less than 98% charged), supplements the HFC during extra power requirements as well as very low power requirements (the HFC is inefficient below a certain power level – 7.55% of the total) and is only charged via the HFC when the state of charge (SOC) is less than 50%.

Charging the battery through regenerative braking instead of the HFC increases fuel economy. From this study it is seen that the HFC & battery combination has a slightly lower efficiency when compared to the HFC, SC & battery combination, even though the weight of the former system is significantly less. An advantage of the HFC & battery combination is that it is more cost effective due to the absence of the SCs and the bidirectional DC-DC converter. A major disadvantage is that the battery life is much shorter than that of the HFC, SC & battery combination as the battery is continuously charged/discharged throughout the operation of the vehicle.

Thoungthong et al. [22] utilizes a proton-exchange membrane fuel cell (PEMFC) of 500 W, 40 A, 13 V is combined with a lead-acid battery of 33 Ah, 48 V to supply a HFC vehicle. The HFC will utilize a boost converter to optimize the characteristics and boost the output voltage to that of the battery. The battery will not use a converter in order to minimize costs and improve efficiency of the system. The HFC will be the main energy source and when the power demands are large, decrease below the specified level of the HFC or regenerative breaking energy is present in the system the battery will be utilized. This configuration leads to a significant degradation in the battery lifetime, as the battery is constantly supplementing the HFC there is no method to improve this issue without altering the setup (i.e. the use of an additional SC bank to rather supply the peak power demands). The HFC is also used to recharge the battery throughout the operation. This system does improve the efficiency and fuel consumption of the HFC however it leads to an additional consideration in lifetime of the battery as this is significantly reduced due to the charge/discharge of the battery throughout the operation of the system.

The combination suggested by Bauman et al. [21] consisted of a battery pack used in conjunction with an HFC; the former used when there is a high-power demand and the latter as the main source of power. It can also be seen from this configuration that the battery will receive the surplus energy that is not absorbed by the load during low load power. The system worked well with the exception of equipment having lower precision than desired causing a higher error rate and, on occasion, the incorrect operation of the hybrid power system. The system had an overall high efficiency (>90%) with lower hydrogen fuel consumptions.

2.1.2. Hydrogen fuel cell and supercapacitor combination

The combination of the HFC & SC has had a few previous studies and experimental combinations, but all had some form of a limitation, these limitations will be of importance in this experiment. Bauman et al. [21] utilizes a 35 kW HFC combined with a SC bank to supply a HFC vehicle. The HFC utilizes a boost DC-DC converter to increase its voltage to that required by the motor (250–400 V) such that a smaller HFC can be used to reduce vehicle mass and overall costs. The SC bank consists of 27

SC-packs are used in series comprising of six 2.5 V, 350 F cells in series, thus 405 V, 2 F capacity. The SCs do not use a DC-DC converter in order to reduce costs and weight of the system and improve efficiency. The SCs store the regenerative braking energy and only provide extra power when it is required (during accelerations). Best fuel economy is achieved when the sum of kinetic energy in the vehicle and the potential energy of the SCs is kept constant. This study shows that the HFC & SC combination cannot compete with the HFC & battery combination as the SC bank does not have enough energy storage to provide for the peak power requirements. It is suggested that a few SC banks be combined in parallel to increase the energy storage capabilities, however, this increases the weight of the system tremendously decreasing fuel consumption to an infeasible point lower than the HFC & battery combination.

Thoungthong et al. [22] utilizes a PEMFC of 500 W, 40 A, 13 V combined with a SC bank of 292 F, 500 A, 30 V to theoretically power a HFC vehicle. The HFC will utilize a uni-directional boost converter while the SCs will utilize a bi-directional converter to facilitate the power requirements and the storage of the regenerative breaking energy. For this setup, the HFC will be the main supply of power and when peak power demands are observed or regenerative breaking energy is increased above 0, the SC bank will be utilized. The HFC will also be used to recharge the SCs throughout the operation. This setup does allow for HFC downsizing, increased efficiency characteristics as compared to only HFC use and energy recovery through regenerative breaking. The downside of using only SCs as the auxiliary power source is that the system could malfunction during start-up as the HFC requires 5–10 min of constant power. For both of these case studies the future adjustments would be to either increase the SCs energy characteristics or to look into a hybrid system that includes the use of a battery to absorb the bulk of these constant power requirements.

2.1.3. Hydrogen fuel cell, battery and supercapacitor combination

Fewer studies have been done into the use of the power sources in this combination than in the prior two combinations. These case studies will be used to assess the viability of the combinations as well as defining some limitations observed leading to room for improvement.

Bauman et al. [21] utilizes a 35 kW HFC combined with a SC bank (405 V, 2 F) and a Li-ion battery (346.5 V) to supply a HFC vehicle. The HFC utilizes a boost converter such that the HFC required can be smaller and thus more cost effective and the battery will use a bi-directional converter in order to be recharged while the system is in use. In order to minimize mass of the system it is determined that only one of the additional power sources (batteries or SC) will use a converter. The SC will be used to supply power only during peak power requirements and will accept regenerative braking energy only if the SCs are below 400 V; the batteries will continuously supplement the HFC during normal operation, will also be used to store regenerative braking energy (when the SCs don't) and will also be used when the power requirements are too low for the HFC ($<$ 7. 55%), thus, the bi-directional converter is chosen to be used in conjunction with the batteries for its charge/discharge.

The SCs are used to lengthen the lifetime of the batteries and are therefore monitored to remain within the required 250–400 V of the load motor. One major advantage of this setup is that the degradation of the battery is delayed due to it not undergoing high current charge/discharges. The battery in this setup is only used for peak power when the SC is discharged, whereas it is used for all peak power requirements in the HFC & battery combination. This setup does have the downside of being much heavier (due to the SC pack addition) and also more expensive (due to the addition of the SCs and the bidirectional converter), however, it still has a lower fuel consumption compared to that of the HFC & battery setup.

Thoungthong et al. [22] utilizes a combination of a HFC – used as the main source of power, batteries – used to provide boost power over moderate durations and SCs – providing a fast acting source to smooth rapid transients and reduce the degradation of the HFC and battery. This system was tested using a flight simulator in order to get a desired flight profile and performed adequately during all stages of the simulation. These sources are used in conjunction to supplement each other. The battery removes a significant load off of the HFC allowing the HFC to have a much lower voltage drop throughout the simulation. The SC allows for a much smoother power curve providing significant energy absorption to the system. Thus, it provides considerable load smoothing to the HFC and has the expected benefit of increasing the lifetime and durability of not only the HFC but also the battery.

2.2. Experimental setup

The general concept for the proposed experiment will be explained using the conceptual flow diagram shown in Figure 1. The shaded blocks represent the main focus of this experiment – the SCs, controller, DC-DC converter and load switch. The HFC system to be used contains its own DC-DC converter and controller – this existing controller controls when the HFC requires a power supplementation as well as controlling the operation of the HFC, therefore, this controller will not be altered and an additional controller will be used to control the auxiliary circuit (shaded blocks). The solid lines represent the flow of power within the circuit while the striped lines represent the flow of control (either measurements or signals).

The controller receives the power requirements from the programmable load which is used to control the load switch (ON or OFF) – this switch remains closed (ON) for the majority of the tests as it is only desired to remotely control when the SCs are available for certain tests (further explained in section 2.3.4). The SCs send a signal of SOC to the controller which is used to calculate the duty cycle required for the desired output of the DC-DC converter, this duty cycle is sent as pulse width modulation (PWM) signals to control the converter.

The existing HFC system has a constant voltage rating and it is desired to match the SCs voltage with this rating; as the SCs deplete their voltage decreases to a level below this required voltage; to avoid this, a DC-DC converter will be used to boost the voltage of the SCs, to that of the HFC system. The DC-DC converter will also be used to limit the current provided by the SCs to the converter's capabilities. The DC-DC converter will be uni-directional such that the SCs can only provide power and not use it. The HFC system will be used to supply the load and when the load has a power requirement above that which the HFC system can provide, the SCs will be utilized. For the initial tests there will be no control over the use of the SCs (the load switch will be closed), thus allowing them to continuously contribute to the load when required. For a more detailed discussion of the operation Figure 2 will be used. The solid lines indicate power transmission and the striped lines represent signal transmission.

The programmable load was programmed to repeat a specified load (see subsection 2.4 for a detailed discussion). The current requirements of the load were measured using a current sensor placed between the HFC and the load and sent to the microcontroller (Arduino); the HFC controller determined the use of the buffer battery to supplement the HFC. The current measurement sent to the microcontroller was used to determine the switching of the relay (further discussed using Figure 3 and section 2.3.4). The SOC of the SC bank was sent to the microcontroller to be used to determine the PWM signal of the DC-DC converter. Dependent on the configuration, the SC bank was used either with or without the inclusion of the DC-DC converter, these configurations are discussed in section 2.3.4.

Figure 3 shows a functional flow diagram. Here, a relay was used to select when the SC bank was required to supplement the HFC system in supplying the load. This relay was switched using an Arduino, which simply read the value measured by the current sensor and, if determined to be $>$ 7 A, the Arduino would send a signal to the relay to engage the coil and allow current to flow from the SC bank to the load. This selection was only used for a specific configuration discussed in section 2.3.4, for all other configurations the relay remained engaged.

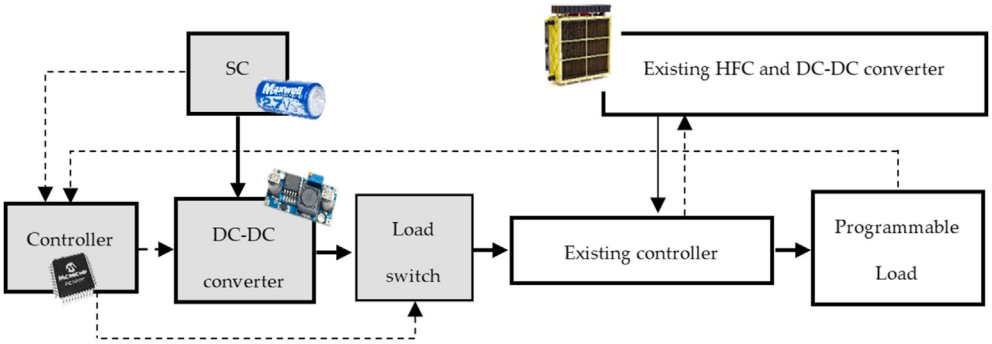

Figure 1. Conceptual flow diagram.

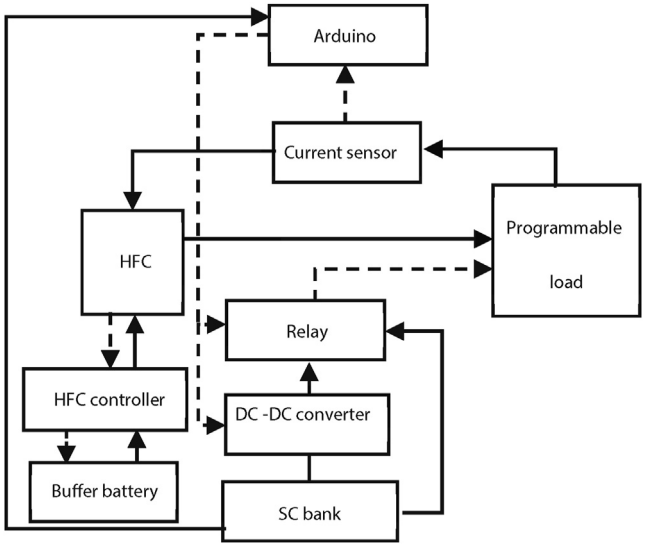

Figure 2. Operational flow diagram.

2.3. Power sources

This research comprises the combination of three power sources in different configurations, in order to assess the effect of each on the output. The research includes the use of an HFC, a SC bank and a LiPo battery. Each of these sources has their respective capacities for the combination, as is explained below.

2.3.1. Hydrogen fuel cell

A 1 kW HFC system obtained from BMPower [23] was available for use. It was initially tested with the original full load profile of maximum 1.2 kW. The HFC system has the capability of providing 1 kW at 50 V. It can also be combined with a LiPo battery, used as the buffer battery (it is used to supplement the HFC when the HFC requires assistance). The available HFC system has a controller that determines the use of the buffer battery and controls the operation of the HFC. For purpose of this experiment the HFC will be used in combination with the LiPo battery and existing controller as one system.

2.3.2. Lithium polymer battery

The battery pack used to supplement the HFC consists of two 12 s LiPo batteries, each with a weight of 0.4 kg, 50 V rated voltage and energy density 160 Wh/kg. Using these details and Eq. (1) (obtained using a process of elimination and Eq. (19.9) from [24]), the capacity rating of the battery pack was determined. Each battery was calculated to have a capacity of 1.33 Ah, thus 2.66 Ah for the battery pack.

$$Capacity(Ah) = \frac{Energy\ density\left(\frac{Wh}{kg}\right) Weight(kg)}{Nominal\ voltage(V)} \quad (1)$$

2.3.3. Supercapacitor bank

Previous case studies suggest the use of a SC bank that can match the capabilities of the existing system it wishes to be combined with [18, 21, 22, 25, 26, 27, 28, 29]. The existing HFC system contains a buffer battery that supplements the HFC when required. As the SC bank was also used to supplement the HFC, it is desired that it matches the capacity of the buffer battery.

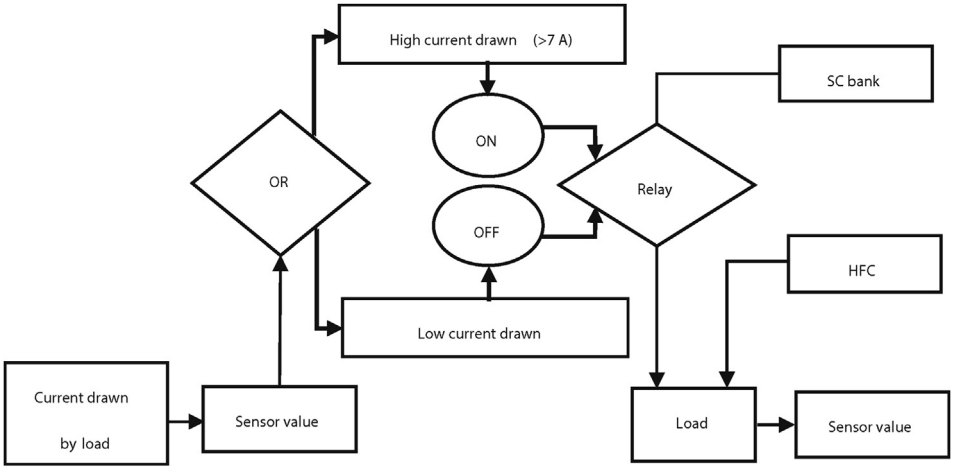

Figure 3. Functional flow diagram.

As calculated, the buffer battery pack has a capacity of 2.66 Ah (maximum voltage 50 V and weight 0.8 kg). If the buffer batteries were to be simply replaced by an equivalent SC bank then these requirements will allow the system to operate in an equivalent fashion without compromising the efficiency thereof [21].

To determine the values of the capacitors, the capacity of the buffer battery pack was converted to the applicable unit in Farad. To achieve this, the capacity rating is first converted to ampere–second, thus converting to Coulomb, using Eq. (2) (adapted from Eq. (19.2) in [24]).

$$Capacity(C) = 3600(capacity(Ah)) \tag{2}$$

Using the capacity rating of 2.66 Ah, the capacity was converted to 9 576 C. Next, the capacitance can be calculated using Eq. (3) (Eq. (18.10) from [24]).

$$Capacitance(F) = \frac{Capacity\ rating(C)}{Voltage(V)} \tag{3}$$

Using the calculated capacity rating and a voltage rating of 50 V, the total capacitance was calculated to be 191.52 F. The nominal voltage of a SC is 2.7 V, thus 19 cells will be required in series to reach 50 V. In series, the total capacitance can be calculated using Eq. (4) (Eq. (6.28) from [30]), which can be rewritten to calculate the capacitance per cell.

$$Total\ series\ capacitance = \frac{capacitance\ per\ cell}{number\ of\ cells} \tag{4}$$

This equation is valid under the assumption that all connected capacitors have the same capacitance; thus the required capacitance per cell will be 3638.88 F. The largest SC available is 3400 F, with a rated voltage of 3 V per cell. With these values, only 17 cells will be required, thus reducing the capacitance per cell to 3255.84 F. Therefore, the 3400 F cells will be sufficient. According to the Maxwell datasheet [31], the weight of one 3 V/3400 F SC cell is 496 g, therefore the combined weight would be 8.43 kg, which is far greater than 800 g.

To solve the weight issue, the system was designed to accommodate SCs that only supply the increase in power above 1 kW. Furthermore, a boost DC-DC converter was used to increase the voltage requirements from a lower level to the desired 50 V. This allowed the SCs to be much smaller and to recharge much faster, hence making the system more efficient. From the load profile, the maximum power consumed is ~1200 W, which is above the 1 kW rating of the HFC. It is at these points above 1 kW that the SC bank will be required.

The system was designed such that the SC bank is utilized twice during the load (to be discussed in section 2.4 and indicated in Figure 5 by the green blocks), with each period lasting 2 s. As SCs have the tendency to provide the bulk of the load, the assumption was made that the average power supplied by the HFC will be ~400 W and the SC bank will need to supply the remainder of the power, namely 650 W for the first instance and 800 W for the second instance.

Calculating the energy requirements, for the first instance of 650 W, 1300 J will be required, and for the second instance of 800 W, 1600 J will be required, giving a total of 2900 J. This value was initially rounded up to 3000 J. It was assumed that this is only 80% of the requirement, thus 100% would require 3750 J .The maximum duty cycle of a boost DC-DC converter is ~70%, thus the SCs will only be able to be boosted with a 70% increase in the maximum voltage. Using V_{out} = 50 V and a duty cycle of 0.7, V_{in} (the minimum required input voltage) is equal to 15 V.

However, SCs have an allowable voltage drop, for efficient lifetime usage, of 20%, therefore the 15 V will be the 80% SOC of the SC bank, at which the converter will be able to boost the input voltage for the entire 20% discharge of the SC bank; 100% SOC of the SCs will therefore be 18.75 V. To achieve this total voltage, about seven cells of 2.7 V each were required—this value is rounded up to eight cells. The maximum voltage will be 21.6 V and the minimum will be 17.28 V. To determine the required capacitance of the SC bank, Eq. (5) is used.

$$C = \frac{2(energy(J))}{V^2} \tag{5}$$

The 3750 J, calculated earlier, is the energy required at the output of the DC-DC converter. Using the law of energy conservation and the efficiency of the system, the output energy of the converter will be a percentage of the input energy. This percentage is the efficiency of the converter (assumed to be 90%). This 10% difference is due to power losses occurring in a system. Therefore, the required input energy was determined using Eq. (6) (Eq. (6.10b) from [24]).

$$E_{in} = \frac{E_{out}}{\eta} \tag{6}$$

For this equation, η refers to the efficiency constant of 0.9 and results in a minimum required energy at the input of 4167 J. Using this energy requirement and the minimum voltage of the input (80% of the SC bank maximum voltage—mentioned earlier as the most efficient SC operating range), the total capacitance was calculated and rounded up to 28 F. The minimum voltage of the SCs is used as this will ensure that the SCs have sufficient energy for the requirement, for the entire range of discharge. Using Eq. (4) and eight cells, the capacitance per cell was calculated to be 224 F.

To verify that this value is correct, the energy it can supply was calculated and compared with the energy requirement of the load profile. The input energy was calculated to be 6532 J (with 28 F total capacitance), which is greater than the 4167 J requirement at the input—thus a value greater than 224 F per cell can be used in the system. For this project, the capacitance per cell was chosen to be 360 F, which delivers 10498 J (more than sufficient to account for losses in the system). According to the Maxwell Technologies datasheet [32], each one of the SCs weighs 71.4 g, giving a total of 571.2 g, which is well under the weight of the two batteries of 0.8 kg, hence leaving sufficient weight for the circuitry.

2.3.4. Configuration

The power sources were tested in multiple configurations in order to assess how each source affects the operation of the system in response to the load. These configurations were also used to compare the results, to determine which is best suited for the application. Before the SC bank was combined with the HFC system, each individual power source's response to the load was required—this allows for a simpler evaluation of the individual contributions when the sources were combined. Three individual tests were initially conducted – the HFC system, the SC bank and the combination of the two power sources.

It was also desired to determine the effect of the DC-DC converter on the SC bank and the system. Therefore, two additional tests were conducted, in which the SC bank was combined with a DC-DC converter. One final test was conducted to show how the addition of selective switching affects the hybrid system. Furthermore, it was also desired to determine whether the order of the connections affected the operation of the system. Two rounds of tests on the six combinations were conducted (to verify the results obtained from each test). The connections for the respective rounds are shown in Figure 4 (use was made of two switches to demonstrate the required connections).

For round 1 (connection 1) the switch 1 was closed while switch 2 remained open. This connection indicates that the sources are connected in parallel with each other and the load, with the load at the end of the parallel connection. For round 2 (connection 2) switch 1 remained open and switch 2 was closed. This connection again indicates that the sources are connected in parallel with each other and the load, but now with the load between the two sources.

To summarize the six combinations – the HFC and SC were tested individually and then as a combination; the SC bank was combined with the DC-DC converter and tested individually and when combined with the HFC; finally, the HFC and SC (with DC-DC converter) were combined using a relay to control the switching.

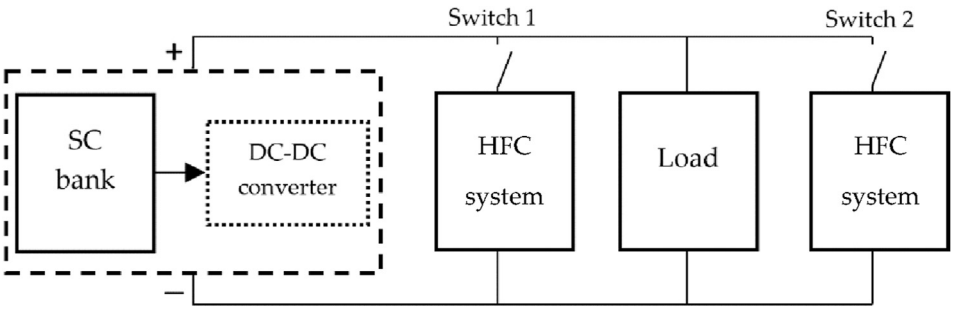

Figure 4. Connections 1 & 2: experimental tests.

2.4. Load profile

The load profile used to assess the operation of the different configurations was obtained from an existing hydrogen drone and reduced to a level that can be used by all the power sources. The original load profile is shown in Figure 5.

In this load profile there is a horizontal line indicating when the proposed system makes use of the buffer battery to supplement the HFC. This occurs when the system requires more than 1 kW of power to operate. The HFC system (including the buffer battery) provided for this experiment has a rating of 1 kW, however, as the HFC is used for research and experimentation in the HySA laboratory at the North West University, through the years of operation the system has degraded to a point where it is suggested to be used to supply a maximum of 450 W. As the system can supply 50 V, this leaves a maximum current supply of 9 A. While testing the new load profile (450 W maximum) it was discovered that with a maximum demand of 9 A from the load, the HFC system supplied a maximum of 350 W, therefore the load profile was initially reduced accordingly to 350 W.

It is suggested in the case studies [21, 22] that the SC bank be used without a DC-DC converter to mainly reduce costs. This project has the future goal of combining SCs into a HFC drone – therefore the experiment is weight and size sensitive. For this experiment it is desired to examine how a DC-DC converter will affect the operation of the SC bank and the entire hybrid system to determine whether it is viable and can be used to reduce the size and weight of the SC bank. Therefore, the point of reference for all the experimentation was chosen to be the SC bank without the DC-DC converter.

The SC bank was designed to have a maximum voltage of 21.5 V. The available HFC has a voltage of 50 V – which is desired to be matched by the SC bank; a smaller HFC is not available for experimentation and the available one is attached to a building supply of hydrogen that is constantly replenished. When the HFC was tested with repetitions of the 9 A (450 W) version of the load profile shown in Figure 5 it was shown that the HFC has an unvarying supply of the load. For this reason it was decided that the HFC would be replaced with a laboratory power supply (LPS) with a maximum 1.6 A, 21.5 V rating. This replacement allowed the unaided SC bank to match the theoretical HFC voltage whilst still obtaining usable and comparable results. As of such the load profile was further reduced to a 3 A, 52 W maximum load shown in Figure 6.

The SC bank was designed for the full 1.2 kW load profile, as it will allow for an easier transition when a larger HFC system is available, and the DC-DC converter was designed for the 3 A load profile as it is desired to be combined with the available HFC system.

3. Simulations

The configurations mentioned above were simulated using Simulink® to assess the validity of the circuit design and proposed experiment as well as to have a basis for comparison against the experimental results. These simulations are provided below. The Simulink® circuit used for the experimentations follows the configuration shown in Figure 4, with the HFC simulated using a Voltage source block and the SC bank using the Supercapacitor block built in to Simulink®.

3.1. Hydrogen fuel cell system

The response of the HFC to the required load is shown in Figure 7.

From the figure it is evident that the entire load was not provided, however, the HFC managed to supply 99.47 % of the load – this deviation

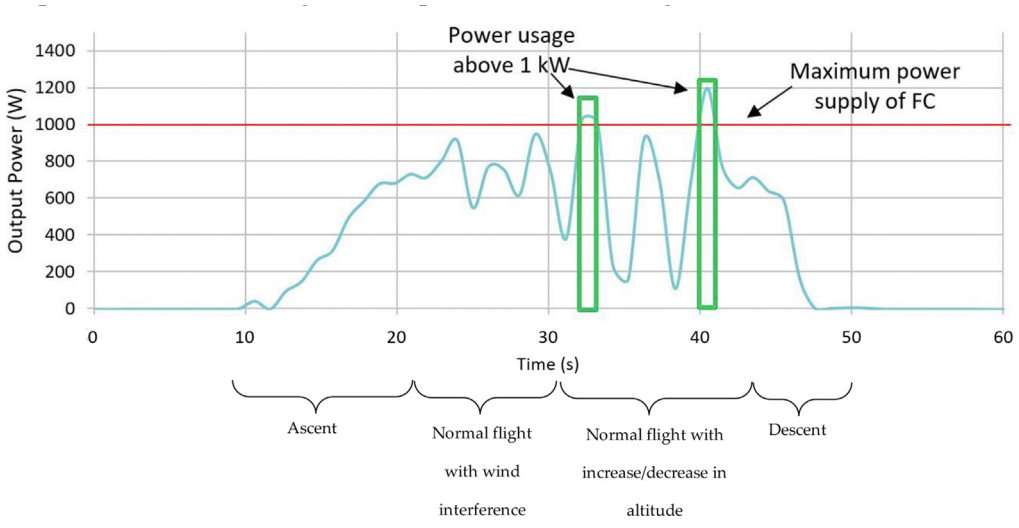

Figure 5. Full load profile (1.2 kW).

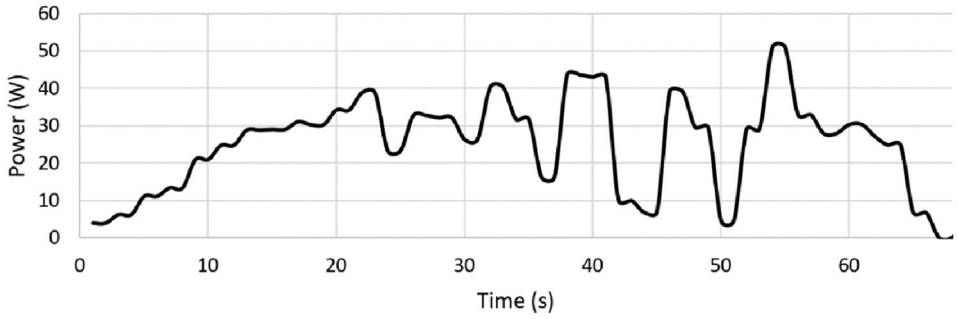

Figure 6. Adjusted 3 A load profile.

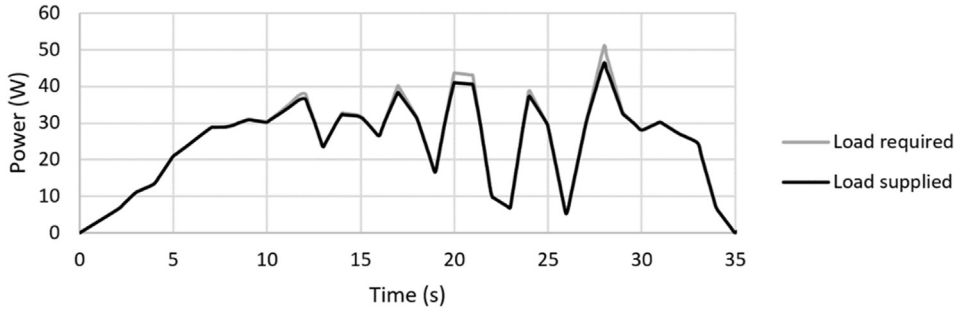

Figure 7. Simulated response of HFC system to 3 A load.

is expected to be provided by the SC bank. In order to determine the duration of the HFC system here and onward, Faradays Law of Electrolysis [33] will be consulted – this loosely states that the hydrogen consumption is proportional to the current drawn. Therefore, to determine the hydrogen consumed, the current drawn for a single repetition will be used in Eq. (7).

$$It = \frac{V\rho Fz}{M} \tag{7}$$

Using this equation the duration of the HFC system is determined to be 268 s.

3.2. Supercapacitor bank - unaided

The response of this system to the load is shown in Figure 8.

It is evident from the figure that the load is initially provided whereafter the provision decreases for each repetition according to the depletion of the SC bank. The load was repeated until the SC bank reached the recommended 80% SOC – found to be after 190 s with the required load being provided with an efficiency of 90.69% for this duration. The SC bank achieved a 99.99% efficiency for the first repetition – this is 0.53% better than the HFC.

3.3. Supercapacitor bank with DC-DC converter

The response of this combination to the 3 A load is shown in Figure 9.

The response shown is that measured at the output of the DC-DC converter. The load was repeated until the SC bank reached 80% SOC – after 186 s for this duration the load was supplied with 91.58% efficiency. This lack of provision is evident from the figure and results in the assumption that the DC-DC converter does not improve the performance of the SC bank – it decreases the usable time and the measured efficiency.

3.4. Hydrogen fuel cell-supercapacitor system – unaided

The response of this combination to the load is seen in Figure 10.

The individual contribution of each source as well as the combined contribution to the load is shown for the duration of the load. This combination delivered an efficiency of 99.99% - the required and combined supplied load lie on top of each other in the figure. It is apparent that the HFC is providing the bulk of the load with the SC providing the jumps in load above that which the HFC can supply.

It is seen in the figure that the graph of the power supplied by the SC extends into the negative region of power – this shows that the SC bank is receiving power from the HFC. This is expected as there is no method of blocking the flow of current towards that SC bank in this configuration

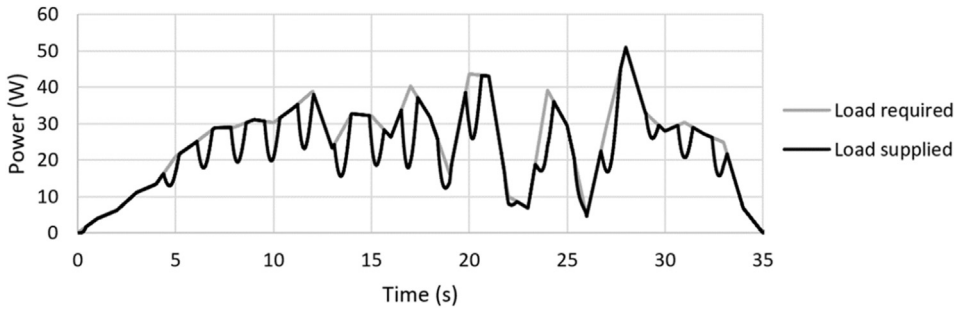

Figure 8. Simulated response of unaided SC bank to 3 A load.

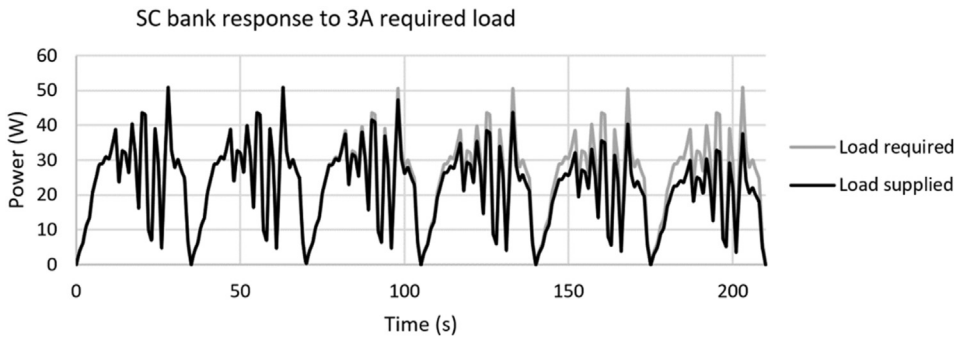

Figure 9. Simulated response of SC bank with DC-DC converter to 3 A load.

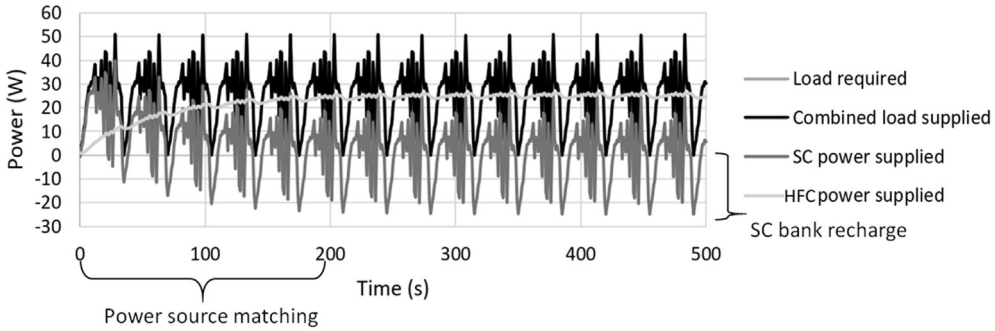

Figure 10. Simulated response of HFC-SC unaided combination to 3 A load.

and as such as it depletes it starts absorbing power in order to recharge. The duration of this system was determined using Eq. (7) as 249.75 s. As the HFC system continually recharges the SC bank it will only drop to 80% SOC when the HFC is depleted to the point where it can no longer provide for the SC bank. Therefore the duration of this combination is seen as the duration of the HFC.

3.5. Hydrogen fuel cell-supercapacitor system with DC-DC converter

The response of this configuration to the 3 A load is shown in Figure 11.

The individual contribution of each source can be seen above with the combined contribution having a 99.91% efficiency in providing the required load. Using Eq. (7) the duration of the HFC is determined to be 403 s while the SC bank has a duration of 428.08 s – therefore the system has a duration of 403 s. As the DC-DC converter is bidirectional it blocks the current flow toward the SC bank therefore not allowing it to be recharged by the HFC. It is evident from the figure that the HFC provides the bulk of the load with the SC bank providing the increase in power at the peak requirements of the load.

3.6. Hydrogen fuel cell-supercapacitor system with DC-DC converter and selective switching

The response of this system to the load is seen in Figure 12.

For this combination a relay was set to only allow the SC bank to provide power when the power needs exceeded ~35 W. It is shown in the figure that at these points the HFC initially supplies drops to supply no load – this can be attributed to the SCs very low internal resistance (3.4 mΩ) and willingness to supply the entire load. For the duration of the load – calculated as 293 s using Eq. (7) (293 s for the HFC and 2265 s for the SC bank) – the system achieved a 99.66% efficiency.

4. Experimental results

4.1. Hydrogen fuel cell system

The available HFC system that was used in the experiments is shown in Figure 13, the dimensions of which can be obtained from the datasheet [23]. This system is supplied by a hydrogen source connected to the building where it is stationed, thus the hydrogen supply was constant.

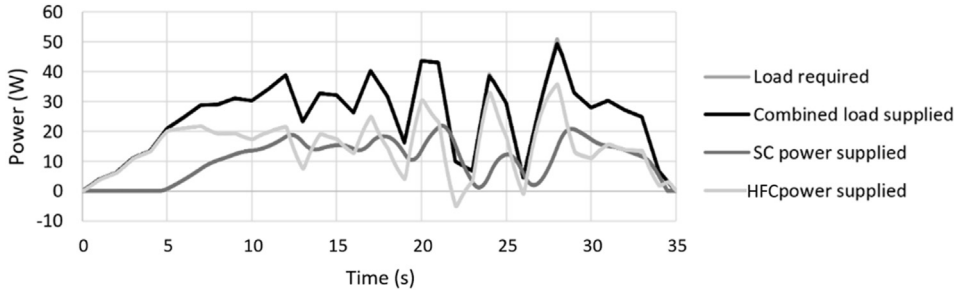

Figure 11. Simulated response of HFC-SC-DC-DC converter to 3 A load.

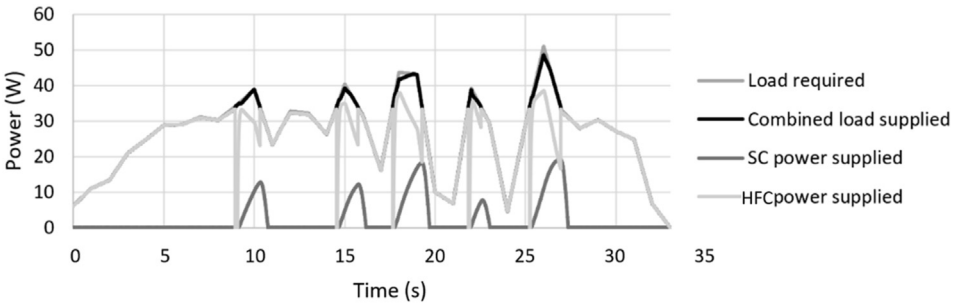

Figure 12. Simulated response of HFC-SC-DC-DC converter with selective switching to 3 A load.

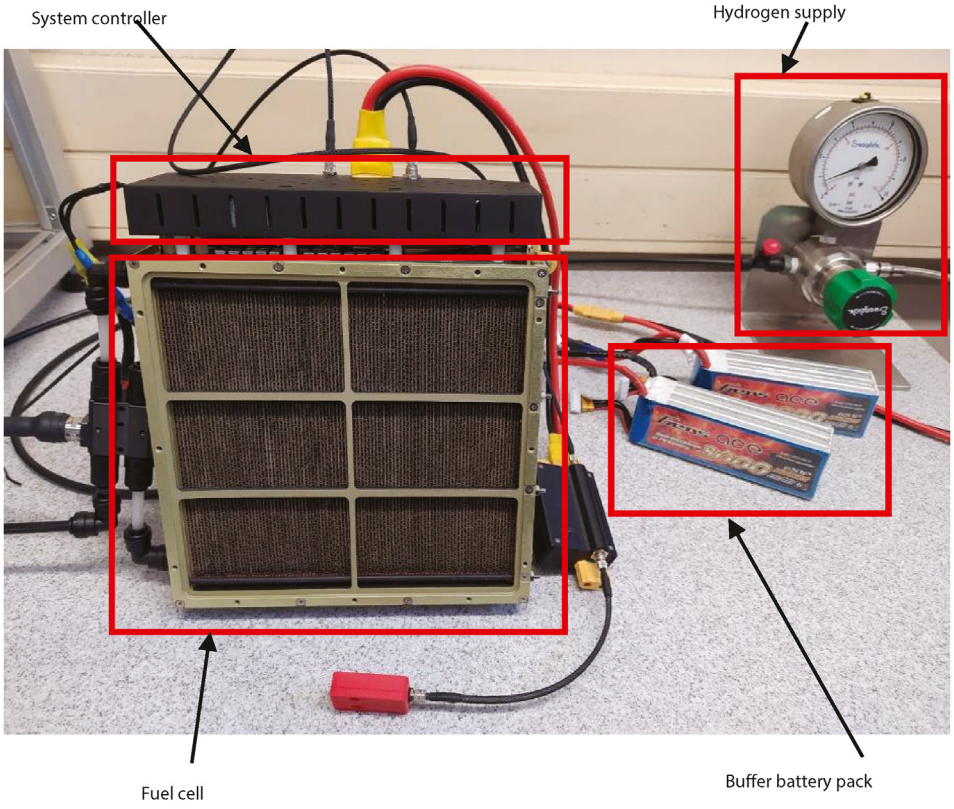

Figure 13. HFC system used for experimentation.

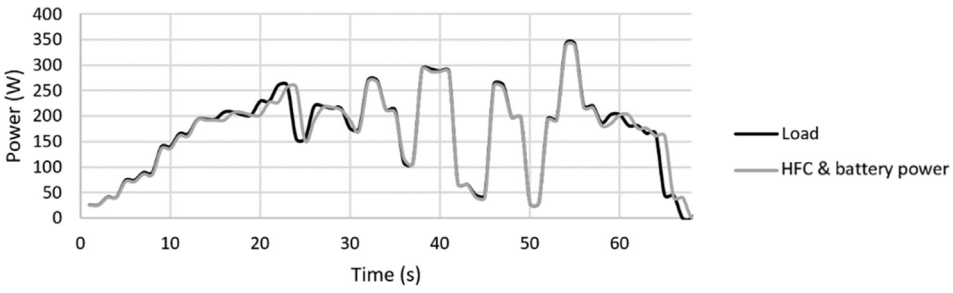

Figure 14. Experimental response of power supplied by HFC system to 9 A load.

The available HFC system was tested using a reduced 9 A load as it was degraded, such that it had a maximum deliverance of ~350 W (explanation provided in section 2.4). Therefore, the 1.2 kW load was reduced equivalently and used to test the HFC to determine its response to the load, shown in Figure 14.

It is evident that the HFC system provided the power required by the load with a calculated efficiency of 99.62%.

It was however desired to combine the SC bank with the HFC system without the use of a DC-DC converter. The requirement here is that the SC bank matches the voltage level of the HFC, or vice versa. A boost DC-DC converter was used with a maximum current capability

of 3 A (new load as explained in section 2.4). The designed SC bank had a voltage of 17.28–21.6 V. Thus, to keep within the 3 A constraint, the SC bank can supply a maximum of 51.84 W at its lowest voltage. For this reason, the HFC needs to have a lower capability. However, the available system cannot be reduced to this point.

Hence it was decided that the HFC system be replaced with an equivalent power source. An LPS was selected as it provided the reduced requirements of 1.6 A at 21 V (both the SC bank and LPS were used with a maximum of 21 V, for consistency, throughout). Before the HFC was replaced with the LPS it was tested with its maximum capacity using the 350 W load such that it could be determined that the LPS replacement is justified. Data in Figure 15 is used for this justification purpose.

It is evident from the figure that the voltage and current supplied by the HFC system, throughout the duration of the load, remained constant. This therefore justifies the use of an LPS as replacement as it will supply the same constant output.

As the SC bank had a maximum current capability of 3 A, the load profile was further reduced to a maximum of 3 A and 51 W for the remainder of the tests. With the replacement of the HFC system, it was desired to see its response to the reduced load of 3 A. Results are shown in Figure 16.

It is evident that the HFC replacement can supply a maximum of ~29 W, with a minimum voltage of 17.5 V this gives a maximum current of 1.66 A. With the alterations, this system now had an endurance of 168 s.

4.2. Supercapacitor bank

The SC bank was tested under two sets of conditions, with and without the DC-DC converter, to show how the DC-DC converter affected its operation. The system used to conduct the remainder of the tests as well as the SC bank system built (experimental setup used for carrying out tests) is shown in Figure 17.

4.2.1. Without DC-DC converter

The SC bank was directly connected to the load and the load was repeated until the SC bank reached its maximum SOC decrease of 20% (at 17.5 V). The response of this connection is shown in Figure 18.

This combination shows a deviation in the power deliverance with a calculated efficiency of 97.21% lasting 130 s.

4.2.2. With DC-DC converter

The SC bank was first connected to the DC-DC converter and then to the load. The load was once again repeated until the SC bank reached its 80% SOC value. The response is shown in Figure 19.

This combination shows a similar deviation in the power deliverance but has a calculated efficiency of 96.6% lasting 125 s. The difference can be attributed to the power losses through the DC-DC converter, which is synonymous with its efficiency.

4.3. Hybrid combinations

Moving on to the consideration of 'hybrid combinations', the three power sources were combined and then tested in three combinations first, without using the DC-DC converter; second, using the DC-DC converter; and, finally, with a method of selective switching. The two rounds of different configurations described in section 2.3.4 will be discussed in cases where notable variances were observed.

4.3.1. Without DC-DC converter

Here, use was made of both connections 1 and 2 (see section 2.3.4), for which similar results were recorded. The results from connection 2 were then used to show the response of the system to the load. See Figure 20.

The figure shows each individual power source's contribution to the supplied load – where the system was able to provide the required load with a calculated efficiency of 97.09% and an endurance of 160 s. Here, for this combination, the SC bank has a negative power component, which is indicative of the SC receiving power from the HFC replacement. This occurs due to the system having no method of blocking power towards the SC bank; thus, when its voltage dropped below that of the HFC replacement, the SC bank was recharged. This caused the HFC replacement to use more energy to supply both the load and the SC bank.

4.3.2. With DC-DC converter

For this configuration, both connections 1 and 2 were used, for which similar efficiencies were recorded, in terms of providing the load. The response of connection 2 is shown in Figure 21.

It is evident that both sources are supplying the load – with the HFC supplying the bulk and the SC bank supplementing. A calculated efficiency of 96.25% was achieved. No significant difference in the efficiencies of both the connections was observed; however, connection 1 reached a significantly greater endurance of 365 s in comparison to the 214 s obtained from connection 1.

4.3.3. With DC-DC converter and selective switching

For this hybrid combination, the SC bank was isolated from the HFC replacement and load for the majority of the load; it was only used when the current requirement exceeded the limits of the HFC replacement (as discussed in section 2.2). For this isolation, a relay was used, with control via an Arduino and current sensor. The response of this system to the load exhibited no notable difference in the two connections. Thus the response of connection 2 was evaluated. See Figure 22.

Here, both power sources were used to supply the load and a calculated efficiency of 94.29% was achieved with a measured endurance of 223 s. It is also observed that the HFC supplied the bulk of the load and the SC bank supplemented during peak power demands.

5. Discussion

The results obtained from the respective combinations were processed and then combined into Table 1. The content of this table will be

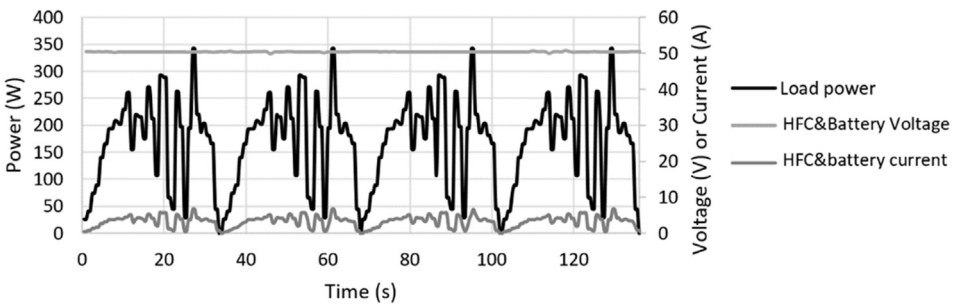

Figure 15. Analysis of voltage and current supplied by the HFC system against power demand of 9 A load.

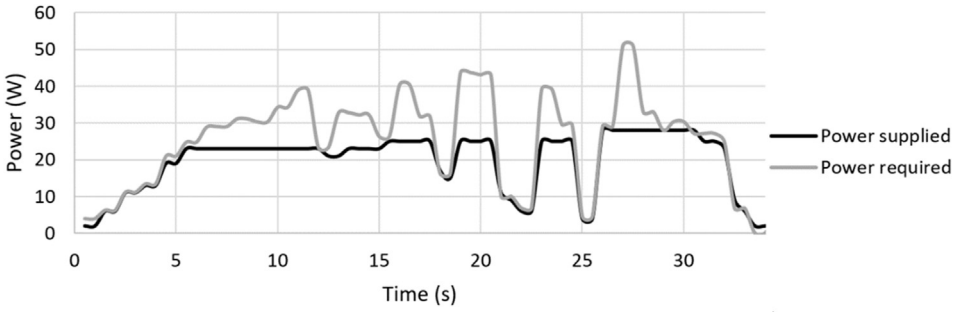

Figure 16. Experimental response of power supplied by HFC replacement to 3 A load.

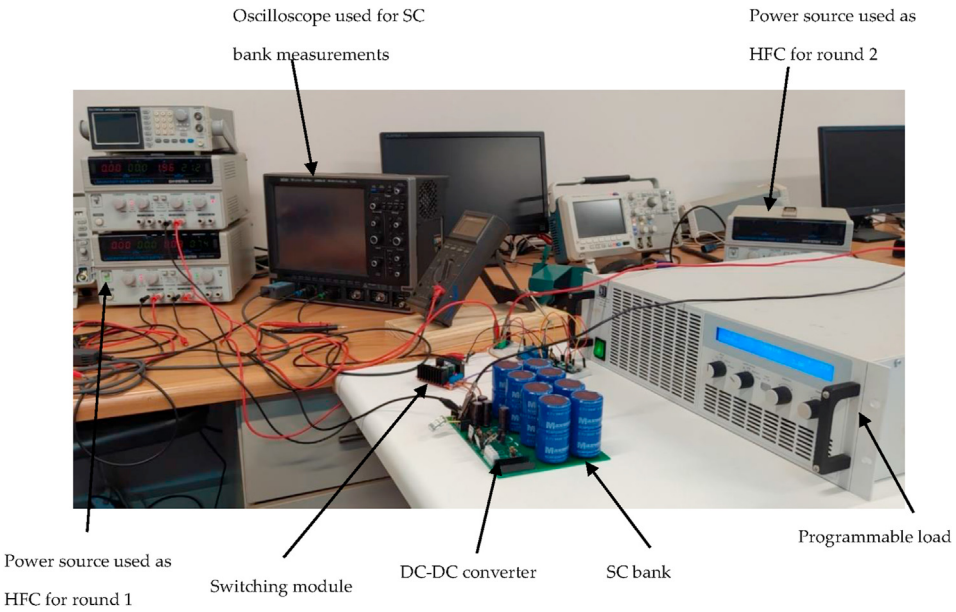

Figure 17. Experimental setup used for testing.

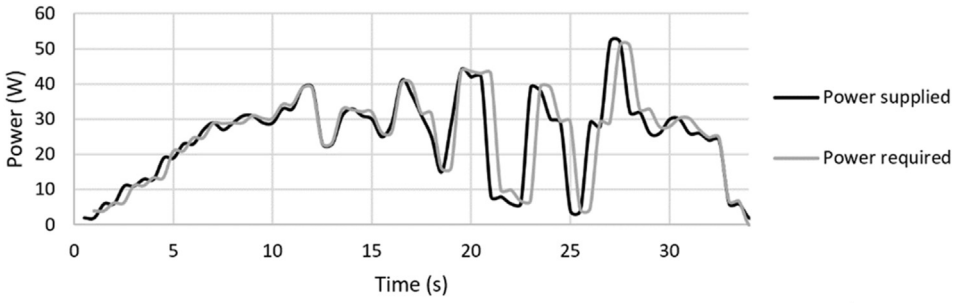

Figure 18. Experimental response of power supplied by SC bank excluding DC-DC converter to load.

used to compare the different combinations to each other as well as to the results obtained through the simulations.

For each combination the weight, power provided, peak power deliverance, energy provided, efficiency and duration has been provided for comparison between the combinations. For combinations with multiple sources, the energy division has been included. The efficiency of each system has been calculated using the power provided expressed as a percentage of that which was required by the load. The peak power deliverance refers to the system's ability to provide the power required at the two instances mentioned in section 2.3.3, as these were initially used to design the SC bank.

In order to compare the different combinations, a point of reference was required – here, three repetitions of the load was selected. The reason for this selection is that the SC bank without a DC-DC converter has a maximum SOC drop over three repetitions, thus all values from the table have been averaged for three repetitions of the load.

The values of the SC bank in the 'SC contribution' column refer to the energy measured at the output of the DC-DC converter, where applicable. To determine the total energy component provided by each combination that includes the DC-DC converter, the efficiency of said converter is required. As measurements of the SC bank's operation had been recorded, the energy is known at the input of the converter; thus, multiplying the latter energy with the efficiency of the converter gives their contribution

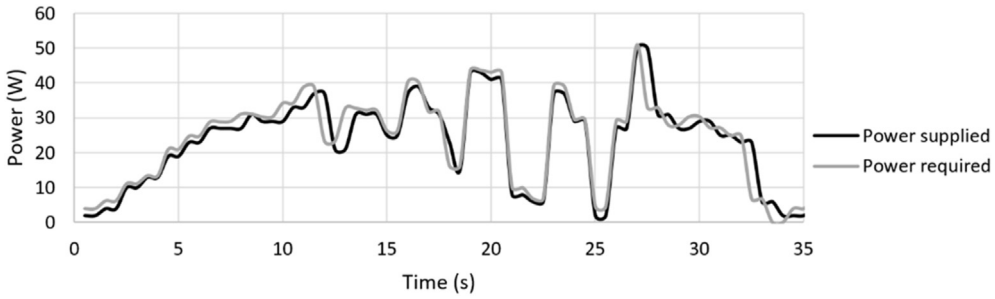

Figure 19. Experimental response of power supplied by SC bank including DC-DC converter to load.

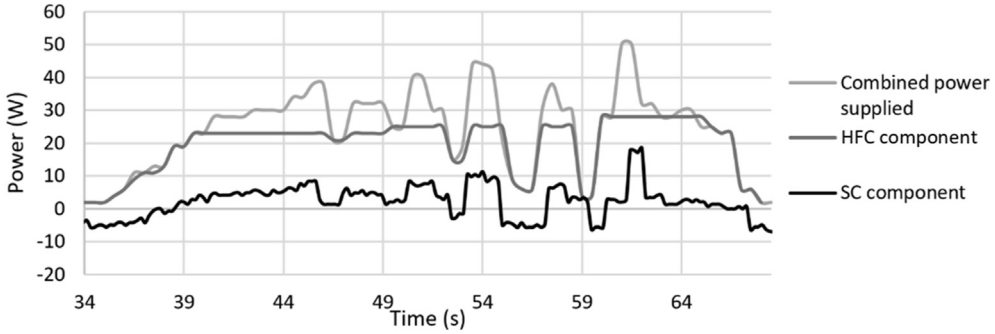

Figure 20. Experimental response of individual sources of hybrid system 1 to the load.

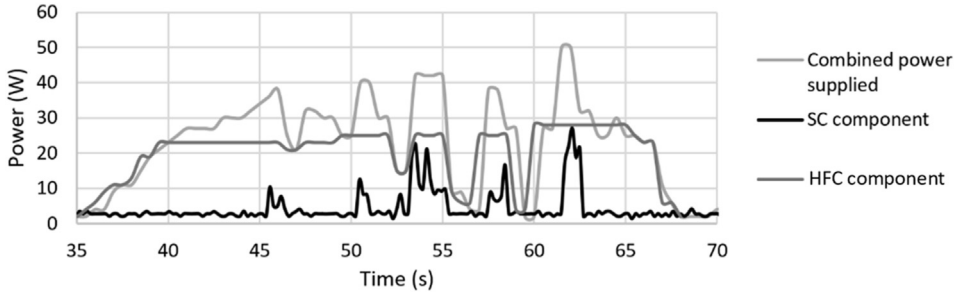

Figure 21. Experimental response of individual sources of hybrid system 2 to the load.

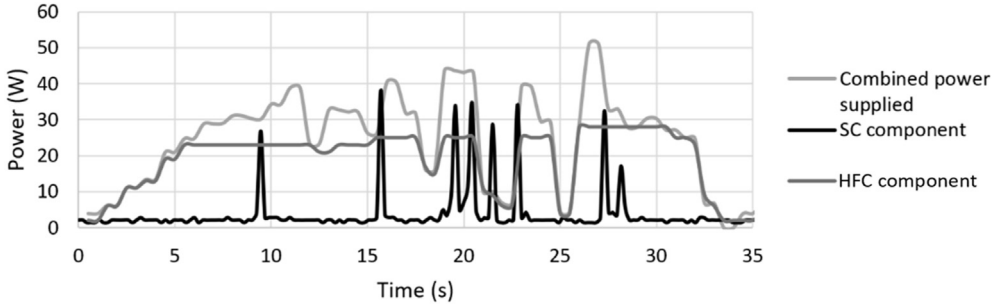

Figure 22. Experimental response of individual power sources of hybrid system 3 to the load.

to the total energy. The efficiency of the converter was calculated as 94.96%.

The final column refers to a simple sensitivity analysis that has been conducted to determine the percent deviation between the experimental and simulated results. For this, the difference between the results is expressed as a percentage of the simulated results.

The SC bank with converter test shows that the DC-DC converter reduced the efficiency and usable time of the SC bank. Hence, it can be deduced that although the converter can reduce the weight of the system it is questionable whether the decrease in efficiency and usable time will nullify this benefit. This deduction is justified based on the similar difference in efficiencies noted between the HFC-SC combinations with and without the DC-DC converter. It was also noted, in the last three combinations shown in the table, that each addition of a component to the systems led to a decrease in efficiency, attributable to power losses of each component and connecting conductors between them.

Table 1. Individual source response.

		Desired	Simulated	Experimental	Sensitivity analysis (%)
HFC system	Weight (g)			1400	
	Efficiency (%)	>90	99.47	76.27	23.32
	Power provided (W)	25.14	28.46	19.51	31.45
	Peak power deliverance (%)	100	98.41	67.99	30.91
	Energy (J)	857.14	852.60	653.74	23.32
	Duration (s)		268	168	37.46
SC	Weight (g)	<800		571.2	
	Efficiency (%)	>90	99.99	97.21	2.78
	Power (W)	25.08	23.93	24.68	3.13
	Peak power deliverance (%)		99.99	97.79	2.20
	Energy (J)	840.27	837.65	828	1.15
	Duration (s)		190	130	31.62
SC-DC-DC	Weight (g)			700	
	Efficiency (%)	>90	91.58	96.66	5.55
	Energy at DC-DC input (J)	933.64	657.39	850.24	29.34
	Energy at DC-DC output (J)	840.27	577.97	808.43	39.87
	Power provided (W)	24.76	22.67	24.13	6.42
	Peak power deliverance (%)		90.80	97.36	7.22
	Duration (s)		186	125	32.77
SC-HFC	Weight (g)			1900	
	Combined Energy (J)	829.54	900.18	820.26	8.88
	SC contribution (J)	663.63	314.70	188.39	40.14
	HFC contribution (J)	331.82	864.55	798.45	7.65
	Efficiency (%)	>90	99.99	97.09	2.90
	Power provided (W)	24.76	24.76	24.49	1.08
	Peak power deliverance (%)		99.99	95.30	4.69
	Duration (s)		250	160	36.00
SC-HFC with DC-DC	Weight (g)			2100	
	Combined Energy (J)	840.34	771.81	811.39	5.13
	SC contribution (J)	504.20	304.85	115.80	62.01
	HFC contribution (J)	336.13	492.46	715.76	45.34
	Efficiency (%)	>90	99.91	96.25	3.66
	Power provided (W)	25.09	25.07	24.22	3.38
	Peak power deliverance (%)		99.54	95.93	3.63
	Duration (s)		403	365	9.43
SC-HFC with DC-DC & selective switching	Weight (g)			2200	
	Combined Energy (J)	841.41	802.40	800.55	0.23
	SC contribution (J)	504.84	40.28	139.97	247.49
	HFC contribution (J)	336.56	714.81	679.04	5.00
	Efficiency (%)	>90	99.66	94.29	5.39
	Power provided (W)	25.12	25.03	23.90	4.53
	Peak power deliverance (%)		98.60	96.92	1.70
	Duration (s)		293	223.43	23.74

It is questionable whether the selective switching is viable as it decreased the efficiency of the system whilst increasing the weight, however, it provided better peak power deliverance and a longer duration. It was mentioned that two rounds of each test were conducted for the HFC-SC combinations and for both rounds all the combinations obtained similar efficiencies and it is thus not necessary to present both results. However, the HFC-SC combination containing the DC-DC converter (without selective switching) obtained a significant variance in the durations between the rounds – round 1 achieved 365 s of operation (with 574 s usable time for the SC bank) whereas round 2 achieved 214 s. This leads to the assumption that the self-regulation of the sources is highly dependent on the order of connection of the sources and can thus be as efficient (if not better) than a method using selective switching.

As the endurance is highly dependent on the usage of the HFC system, to increase endurance the HFC system would need to be used less and the SC bank used more. Therefore, the switching value/point can be adjusted to allow the use of the SC bank at an earlier stage. However, due to the internal resistances of each power source the system decides when each power source is utilized – it is assumed that this endurance is the best that can be achieved with the available power sources.

The first HFC-SC combination shows an improvement in the endurance of the SC bank but a decrease in that of the HFC system – this is attributed to the lack of a current blocking device prohibiting the HFC system from charging the SC bank. When the SC bank is recharged by the HFC system, the HFC system supplies a significantly larger amount of energy in a shorter period of time depleting its capacity faster. This is shown where the combined energy of this combination is smaller than the summation of the energy provided by the two contributions.

It is also seen that all the HFC combinations with the SC increased the energy supplied in response to the load, not only in the combination but also in the HFC systems' component. Thus, the HFC system (when

combined with the SC bank) responds more efficiently to the required load.

For most of the combinations the results obtained for the efficiency, peak power deliverance and duration was seen to be larger during simulations than experiments, with the exception of the SC-DC-DC combination, where only a longer duration was achieved. This is expected as the simulations cannot account for power losses caused by heat and conductor lengths. The results of the simulations were the similar to that of the experiments with where the HFC-SC with DC-DC converter achieved the longest duration and selective switching was found to have minimal benefits; the addition of components resulted in the combinations having a decrease in efficiency as well as peak power deliverance.

For the sensitivity analysis all the values obtained for the HFC system have such a large deviation (>23%) as the HFC system used for experimentation was of a smaller capacity than that which was required by the load and simulated. This was chosen to be able to see what effect the addition of the SC bank would have. Most of the other categories achieved small deviations (<10%), which is expected, as the simulations tend to use ideal circumstances which are not applicable during physical experimentation (i.e. power losses due to environmental temperatures, conductor losses, etc.), this argument can also be applied to the deviation shown at the DC-DC input and output and the duration deviations of the different combinations.

The SC contributions in the three SC-HFC combinations are seen to have quite a large deviation, one reason for this could be the difference in connecting conductors between the simulations and the experiments and another could be that the applied DC-DC converter has a larger internal resistance than what was used for the simulations. The latter however does not apply to the difference seen in the final SC-HFC combination, where the experimental contribution of the SCs is far larger than that achieved from the simulations. An explanation for this could be attributed to the relay used during experimentation.

During simulations the relay, as well as the SC bank, will behave ideally, whereas, when used in the experiment the relay causes the SC bank to provide a large burst of energy as soon as the relay closes, which is often larger than that which is required by the load. This is due to the low internal resistance of the SCs and is further justified when comparing Figure 21 and Figure 22. In Figure 21 the SC bank is seen to provide a magnitude of power smaller (and for a period of time longer) than that of Figure 22.

The large deviation seen for the HFC contribution of the second SC-HFC combination is attributed to the adjustment required by the HFC during experimentation due to the decreased contribution of the SC bank.

Using the results summarized in Table 1, a Ragone plot was constructed to present the effect of the SC bank on the individual systems used in this experiment. This plot is shown in Figure 23. Comparing this achieved Ragone plot to that of Aravindan et al. [8], it is observed that the experimental HFC system utilizes a buffer battery thus affording it a larger power density and lower energy density – therefore lying in a more central position on the experimental Ragone plot as compared to the referenced Ragone plot.

A further observation is made that the SC bank (with- and without the DC-DC converter) provides a larger energy density than the HFC system in both Ragone plots – this is firstly due to the HFC system replacement chosen having a smaller capacity such that the effect of the SC bank can better be observed and secondly due to the capacity of the SC bank being designed for the available HFC system and full 1 kW load profile.

The DC-DC converter is seen to significantly improve the power density of the system with a larger factor than the decrease caused in the energy density. The graph contains two diagonal lines whose gradient is determined by dividing the y-axis by the x-axis – this delivers the endurance of each combination. It is noteworthy to bear in mind that these densities are calculated using the weight of each system and therefore the endurance is affected by this weight, with the unaided SC bank having the lowest weight of 0.5 kg.

The three HFC-SC combinations fall on the same gradient thus delivering a similar endurance with respect to the weight variance of each (see Table 1). By simply adding the unaided SC bank to the HFC system, the energy- and power densities of the HFC system experience a considerable decrease. When the DC-DC converter is included in the HFC-SC combinations a noteworthy improvement in the densities of the HFC system is observed.

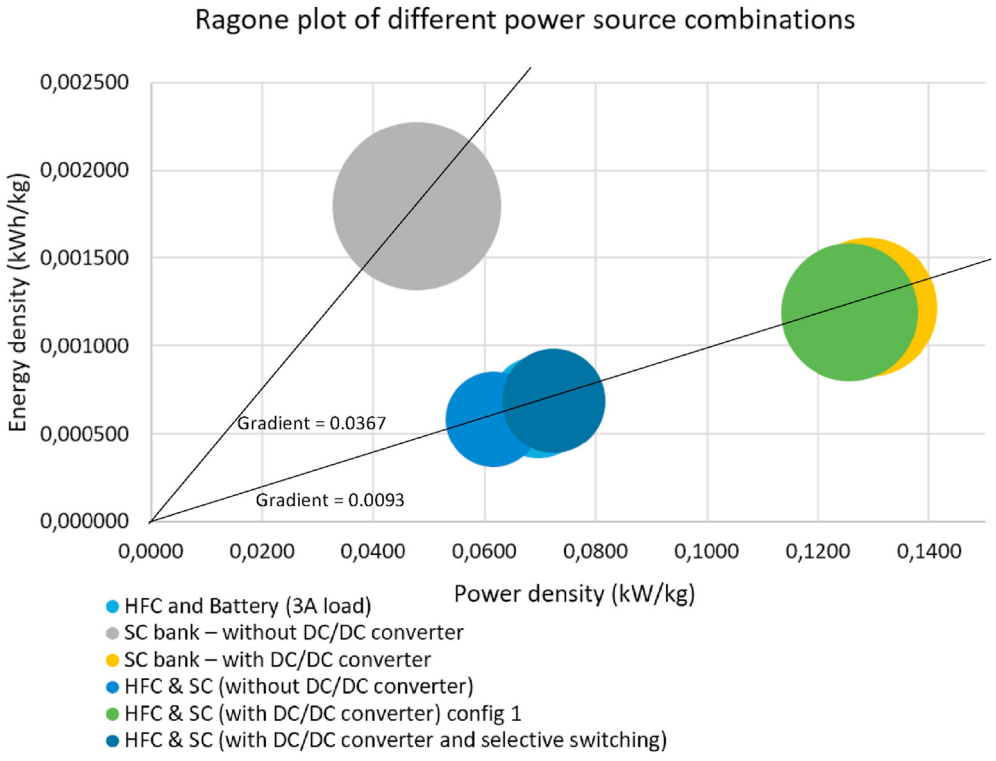

Figure 23. Ragone plot of experimental results.

As mentioned the weight of the system plays a significant role in the calculation of these densities, it is thus understandable that the addition of the SC bank caused a decrease in the densities of the HFC system, however, as the DC-DC converter and switching module add an additional weight to the unaided HFC-SC system, the increase in the densities is of much more interest and is considerably more significant than observed on the graph.

Another noteworthy observation is that of the difference between the densities achieved between the HFC-SC (with DC-DC converter) with and without selective switching. Without selective switching the addition of the DC-DC converter no longer required the utilization of the HFC to recharge the SC bank, resultantly leading to an increase in the duration of the HFC system and both the densities.

The addition of the selective switching element increased the use of the HFC as the SC bank was only utilized at specified instances of the load – thus leading to a large reduction in the usable time of the combination. As the power and energy density are reliant on the usable duration of the system – these too where reduced.

6. Conclusion and recommendations

Two different storage devices were described and used in various experiments with HFCs: an HFC and SC bank. Six different combinations of these sources were implemented and assessed for their viability. The best combination was found to be the HFC–SC combination with the DC-DC converter and without the use of selective switching, when connected with the load between the two sources. The HFC–SC combination with both the DC-DC converter and selective switching was also found to deliver desirable results; however, it is questionable as to whether the selective switching method is redundant. Furthermore, the DC-DC converter had a negative effect on the efficiency of the SC bank. It reduced the usable time by increasing the energy usage of the SC bank at the converter input whilst decreasing the deliverance of said energy to the required load at its output. The inclusion of the SC bank increased the total efficiency of the power source as a whole and allowed the HFC system to function more optimally to provide energy to the system.

The proposed project implemented a DC-DC converter with the SC bank in order to be able to use a smaller quantity of cells to match the buffer battery. This is to reduce costs and the weight of the overall system as it is designed for application on a drone. The DC-DC converter exhibited an efficiency of $>$94% and the optimal hybridized storage system obtained an energy density of 1.19 Wh/kg.

The results of the experiments revealed the following:

- The HFC system's response to the load requirements is improved upon the addition of the SC bank.
- The use of a DC-DC converter reduces the efficiency of the SC bank although it improves the efficiency of the HFC-SC combinations (mainly due to its unidirectional flow characteristics).
- The applied selective switching does not offer any significant improvement.
- The usable duration of the system is highly dependent on the order of connection of the power sources.

On completion of the research described, opportunities for further research and aspects to be considered in efforts to achieve further improvements were identified. These include the following.

- As the DC-DC converter is seen to decrease the efficacy of the SC bank, results should be re-examined at a higher power demand to determine whether the efficiency drop increases and whether the benefit of the reduced weight of the system justifies this increase.
- Here, experiments were conducted using an HFC system that already contains and utilizes a battery for supplementation, thus it was not possible to adjust the use of the battery. It is therefore recommended that an HFC system be considered wherein the use of all three sources can be controlled to further improve/assess the effects thereof.
- To date, the system has only been tested in a theoretical and simulated environment using the load profile of a drone. Its evaluation should therefore be extended, to an actual drone, in order to test the actual operation in a real environment.
- SCs are very useful for storing reverse/negative energy, such as that which is present during braking or when a drone decreases altitude. This was evident in our hybrid test without the DC-DC converter. As this current system was not applied to an actual drone, it is recommended that, if the system is integrated with a drone, this concept be applied – it could lead to a further increase in the usable time. For this application a bi-directional converter could be used that only allows current flow toward the SC bank when the system experiences negative energy from the load.
- The system utilized selective switching when the power exceeded 35 W – this value was seen to be too low to benefit the HFC system and reduce its use. Thus, it is recommended that if selective switching be further investigated that the point of switching be adjusted.
- A mechanical relay was used to apply the selective switching – a solid state Relay could be used to reduce weight and decrease interference in the external circuit caused by the coil.

Declarations

Author contribution statement

Ashleigh Townsend: Conceived and designed the experiments; Performed the experiments; Analyzed and interpreted the data; Contributed reagents, materials, analysis tools or data; Wrote the paper.

Christiaan Martinson, Rupert Gouws & Dmitri Bessarabov: Contributed reagents, materials, analysis tools or data.

Funding statement

This work was supported by DST HySA Infrastructure Center of Competence.

Data availability statement

Data will be made available on request.

Declaration of interests statement

The authors declare no conflict of interest.

Additional information

No additional information is available for this paper.

References

[1] J. Lee, K. Kim, S. Yoo, A.Y. Chung, J.Y. Lee, S.J. Park, et al., Constructing a reliable and fast recoverable network for drones, in: 2016 IEEE Int. Conf. Commun., IEEE, 2016, pp. 1–6.

[2] S. Yoo, K. Kim, J. Jung, A.Y. Chung, J. Lee, S.K. Lee, et al., A multi-drone platform for empowering drones' teamwork, in: Proc. 21st Annu. Int. Conf. Mob. Comput. Netw. - MobiCom '15, ACM Press, New York, New York, USA, 2015, pp. 275–277.

[3] A.M. Jawad, H.M. Jawad, R. Nordin, S.K. Gharghan, N.F. Abdullah, M.J. Abu-Alshaeer, Wireless power transfer with magnetic resonator coupling and sleep/active strategy for a drone charging station in smart agriculture, IEEE Access 7 (2019) 139839–139851.

[4] D. Lee, J. Zhou, W.T. Lin, Autonomous battery swapping system for quadcopter, in: 2015 Int. Conf. Unmanned Aircr. Syst., IEEE, 2015, pp. 118–124.

[5] A. Rucco, P.B. Sujit, A.P. Aguiar, J.B. de Sousa, F.L. Pereira, Optimal rendezvous trajectory for unmanned aerial-ground vehicles, IEEE Trans. Aero. Electron. Syst. 54 (2018) 834–847.

[6] M.L. Fravolini, A. Ficola, G. Campa, M.R. Napolitano, B. Seanor, Modeling and control issues for autonomous aerial refueling for UAVs using a probe–drogue refueling system, Aero. Sci. Technol. 8 (2004) 611–618.

[7] M. Lu, M. Bagheri, A.P. James, T. Phung, Wireless charging techniques for UAVs: a review, reconceptualization, and extension, IEEE Access 6 (2018) 29865–29884.
[8] V. Aravindan, J. Gnanaraj, Y.-S. Lee, S. Madhavi, Insertion-type electrodes for nonaqueous Li-ion capacitors, Chem. Rev. 114 (2014) 11619–11635.
[9] M. Alwateer, S.W. Loke, A.M. Zuchowicz, Drone services: issues in drones for location-based services from human-drone interaction to information processing, J. Locat. Based Serv. 13 (2019) 94–127.
[10] L. Ruan, J. Wang, J. Chen, Y. Xu, Y. Yang, H. Jiang, et al., Energy-efficient multi-UAV coverage deployment in UAV networks: a game-theoretic framework, China Commun. 15 (2018) 194–209.
[11] A. Claesson, L. Svensson, P. Nordberg, M. Ringh, M. Rosenqvist, T. Djarv, et al., Drones may be used to save lives in out of hospital cardiac arrest due to drowning, Resuscitation 114 (2017) 152–156.
[12] S.W. Loke, M. Alwateer, V.S.A. Abeysinghe Achchige Don, Virtual space boxes and drone-as-reference-station localisation for drone services, in: Proc. 2nd Work. Micro Aer. Veh. Networks, Syst. Appl. Civ. Use - DroNet '16, ACM Press, New York, New York, USA, 2016, pp. 45–48.
[13] A. Shukla, H. Xiaoqian, H. Karki, Autonomous tracking and navigation controller for an unmanned aerial vehicle based on visual data for inspection of oil and gas pipelines, in: 2016 16th Int. Conf. Control. Autom. Syst., IEEE, 2016, pp. 194–200.
[14] M. Bacco, A. Berton, E. Ferro, C. Gennaro, A. Gotta, S. Matteoli, et al., Smart farming: opportunities, challenges and technology enablers, in: 2018 IoT Vert. Top. Summit Agric. - Tuscany (IOT Tuscany), IEEE, 2018, pp. 1–6.
[15] G. Ding, Q. Wu, L. Zhang, Y. Lin, T.A. Tsiftsis, Y.-D. Yao, An amateur drone surveillance system based on the cognitive internet of things, IEEE Commun. Mag. 56 (2018) 29–35.
[16] Z.F. Pan, L. An, C.Y. Wen, Recent advances in fuel cells based propulsion systems for unmanned aerial vehicles, Appl. Energy 240 (2019) 473–485.
[17] B. Lee, S. Kwon, P. Park, K. Kim, Active power management system for an unmanned aerial vehicle powered by solar cells, a fuel cell, and batteries, IEEE Trans. Aero. Electron. Syst. 50 (2014) 3167–3177.
[18] T. Das, S. Snyder, Adaptive control of a solid oxide fuel cell ultra-capacitor hybrid system, IEEE Trans. Contr. Syst. Technol. 21 (2013) 372–383.
[19] F. Schroth, Drone Energy Sources – Pushing the Boundaries of Electric Flight, Drone Ind Insights, 2017. https://droneii.com/drone-energy-sources. (Accessed 27 November 2020).
[20] J.R. Meacham, F. Jabbari, J. Brouwer, J.L. Mauzey, G.S. Samuelsen, Analysis of stationary fuel cell dynamic ramping capabilities and ultra capacitor energy storage using high resolution demand data, J. Power Sources 156 (2006) 472–479.
[21] J. Bauman, M. Kazerani, A comparative study of fuel-cell–battery, fuel-cell–ultracapacitor, and fuel-cell–battery–ultracapacitor vehicles, IEEE Trans. Veh. Technol. 57 (2008) 760–769.
[22] P. Thounthong, V. Chunkag, P. Sethakul, B. Davat, M. Hinaje, Comparative study of fuel-cell vehicle hybridization with battery or supercapacitor storage device, IEEE Trans. Veh. Technol. 58 (2009) 3892–3904.
[23] BMPower, BMPower Range of products, n.d. https://bmpower.us/. (Accessed 18 May 2020).
[24] P.P. Urone, College Physics, second ed., Brooks/Cole, Sacramento, California, 2001.
[25] Q. Xun, Y. Liu, E. Holmberg, A comparative study of fuel cell electric vehicles hybridization with battery or supercapacitor, in: 2018 Int. Symp. Power Electron. Electr. Drives, Autom. Motion, IEEE, 2018, pp. 389–394.
[26] W. Gao, Performance comparison of a fuel cell-battery hybrid powertrain and a fuel cell-ultracapacitor hybrid powertrain, IEEE Trans. Veh. Technol. 54 (2005) 846–855.
[27] R.M. Schupbach, J.C. Balda, M. Zolot, B. Kramer, Design methodology of a combined battery-ultracapacitor energy storage unit for vehicle power management, Pesc. Rec. - IEEE Annu. Power Electron. Spec. Conf. 1 (2003) 88–93.
[28] R.M. Schupbach, J.C. Balda, The role of ultracapacitors in an energy storage unit for vehicle power management, IEEE Veh. Technol. Conf. 58 (2003) 3236–3240.
[29] G. Pede, A. Iacobazzi, S. Passerini, A. Bobbio, G. Botto, FC vehicle hybridisation: an affordable solution for an energy-efficient FC powered drive train, J. Power Sources 125 (2004) 280–291.
[30] J.W. Nilsson, S.A. Riedel, Electric Circuits, ninth ed., Pearson, New Jersey, 2011.
[31] Maxwell Technologies, 3.0V 3400F ultracapacitor cell. Maxwell technol inc, 2020, pp. 1–5. https://www.maxwell.com/products/ultracapacitors/.
[32] Maxwell Technologies, 2.7V 360F ultracapacitor cell. Maxwell technol, 2020, pp. 2–3. https://www.maxwell.com/images/documents/2_7_360F_ds_3001963_datasheet.pdf. (Accessed 27 November 2020).
[33] D. Barker, F.C. Walsh, Applications of Faraday's laws of Electrolysis in metal finishing, Trans IMF 69 (1991) 158–162.